Title

Transfer stamping of human mesenchymal stem cell patches using thermally expandable hydrogels with tunable cell-adhesive properties

Authors

Jun, Indong
Bin Lee, Yu
Choi, Yu Suk
et al.

Publication Date

2015-06-01

DOI

10.1016/j.biomaterials.2015.03.016

Peer reviewed

Biomaterials 54 (2015) 44–54

Contents lists available at ScienceDirect

Biomaterials

journal homepage: www.elsevier.com/locate/biomaterials

Transfer stamping of human mesenchymal stem cell patches using thermally expandable hydrogels with tunable cell-adhesive properties

Indong Jun [a], Yu Bin Lee [a, b], Yu Suk Choi [c, 1], Adam J. Engler [c], Hansoo Park [d, **], Heungsoo Shin [a, b, *]

[a] Department of Bioengineering, Hanyang University, 17 Haengdang-dong, Seongdong-gu, Seoul 133-791, Republic of Korea
[b] BK21 Plus Future Biopharmaceutical Human Resources Training and Research Team, Hanyang University, 17 Haengdang-dong, Seongdong-gu, Seoul 133-791, Republic of Korea
[c] Department of Bioengineering, University of California, San Diego, La Jolla, CA 92093, USA
[d] School of Integrative Engineering, Chung-ang University, 221 Heukseok-dong, Dongjak-gu, Seoul 156-756, Republic of Korea

ARTICLE INFO

Article history:
Received 17 November 2014
Received in revised form
5 March 2015
Accepted 9 March 2015
Available online 29 March 2015

Keywords:
Thermally responsive material
ECM (extracellular matrix)
Fibronectin
Hydrogel
Mesenchymal stem cell

ABSTRACT

Development of stem cell delivery system with ability of control over mutilineage differentiation and improved engraft efficiency is imperative in regenerative medicine. We herein report transfer stamping of human mesenchymal stem cells (hMSCs) patches using thermally expandable hydrogels with tunable cell-adhesive properties. The hydrogels were prepared from functionalized four arm copolymer of Tetronic®, and the cell adhesion on the hydrogel was modulated by incorporation of fibronectin (FN) or cell-adhesive peptide (RGD). The resulting hydrogels showed spontaneous expansion in size within 10 min in response to the temperature reduction from 37 to 4°C. The adhesion and proliferation of hMSCs on FN-hydrogels were positively tunable in proportion to the amount of FN within hydrogels with complete monolayer of hMSCs (hMSC patch) being successfully achieved. The hMSC patch on the hydrogel was faced to the target substrate, which was then easily detached and re-attached to the target when the temperature was reduced from 37°C up to 4°C. We found that the transfer stamping of cell patch was facilitated at lower temperature of 4°C relative to 25°C, with the use of thinner hydrogels (0.5 mm in thickness relatively to 1.0 or 1.5 mm) and longer transfer time (>15 min). Notably, the hMSC patch was simply transferred from the hydrogel to the subcutaneous mouse skin tissue within 15 min with cold saline solution being dropped to the hydrogel. The hMSC patch following osteogenic or adipogenic commitment was also achieved with long-term culture of hMSCs on the hydrogel, which was successfully detached to the target surface. These results suggest that the hydrogels with thermally expandable and tunable cell-adhesive properties may serve as a universal substrate to harvest hMSC patch in a reliable and effective manner, which could potentially be utilized in many cell-sheet based therapeutic applications.

1. Introduction

Stem cells derived from a variety of organs or tissues have been investigated as one of the most prominent therapeutic cell sources since they have two remarkable properties: (1) the capability of indefinite self-renewal and (2) pluripotency (the ability to generate many cell types) [1–3]. However, conventional transplantation of stem cells involves syringe-based injection following the process of detachment from the culture plate and resuspension, which is prone to exhibit low engraftment efficiency due to rapid diffusion, limited localization to the host tissue, damage by enzymatic digestion, and shear-induced cell death. In addition, other challenges facing stem cell therapy in a functional recovery of damaged tissue include maintenance of unlimited proliferation of stem cells and selective activation of lineage-dependent cell signaling [4–7].

* Corresponding author. Department of Bioengineering, Hanyang University, 17 Haengdang-dong, Seongdong-gu, Seoul 133-791, Republic of Korea. Tel.: +82 2 2220 2346; fax: +82 2 2298 2346.
** Corresponding author. Tel.: +82 2 820 5804; fax: +82 2 814 2651.
E-mail addresses: heyshoo@cau.ac.kr (H. Park), hshin@hanyang.ac.kr (H. Shin).
[1] Present address: Cardiac Technology Centre, Kolling Institute of Medical Research, University of Sydney, Australia.

http://dx.doi.org/10.1016/j.biomaterials.2015.03.016
0142-9612/

In order to improve the overall therapeutic effects of stem cells, a number of delivery methods using biodegradable materials have been developed with being designed to be implantable with tunable degradation rate, mechanical properties, and cellular affinity [3,8,9]. However, biomaterials occasionally displayed several drawbacks such as insufficient cell recruitment and chronic inflammation by uncontrolled degradation of implants [10–12]. Alternatively, a confluent cell monolayer has been harvested using responsive surfaces that can be transplanted to target tissue with avoiding implantation of biomaterials [13,14].The most common method for this approach uses a poly(N-isopropylacrylamide) (PNIPAAm)-grafted surface on which the cell sheet spontaneously detaches from the surface by thermo-rheological transition of the polymeric chains at a lower temperature (20°C) [14]. In addition, enzymatically-degradable polymers (A6K (arginine6-lysine)), magnetite cationic liposomes, and physical stimuli such as electricity and light have also been employed to harvest cell sheets [15–18].

Despite its therapeutic outcomes in many types of tissue, the process to harvest cell sheet possesses several technical challenges. The reversible detachment of cell sheet on the PNIPAAm-grafted surface is sensitive to the density and thickness of the grafted polymer chains, and thus, it may be difficult to achieve consistent level of surface polymerization in laboratory conditions [19]. The varied affinity of cells onto the PNIPAAm-grafted surface may also cause problems: (1) cells with low affinity takes long culture time to reach a confluent monolayer, and (2) cells with high affinity require longer time for detachment even under reduced temperatures (reportedly requiring >30 min). Cell-instructive cues may be immobilized on the PNIPAAm-grafted surface to modulate lineage-dependent differentiation of stem cells, but at the same time, it may potentially decrease the detachment rate of the cell sheet. Other engineering tools to harvest cell sheets showed some drawbacks such as toxicity of magnetic nanoparticles or enzymes, and low versatility [16,20]. Therefore, a universal approach to effectively control stem cell function and rapidly detach the stem cell sheet is desired.

We and our colleagues previously reported transfer stamping of cell patch using thermosensitive Tetronic®-based hydrogels *in situ* polymerized with a cell-adhesive (arginine-glycine-aspartic acid (RGD)) peptide [21–23]. The cell patch transfer was achieved by rapid cleavage between cell receptors and the cell-adhesive peptide on the hydrogel upon rapid expansion of hydrogels when the temperature is reduced from 37°C to lower one. However, the culture of stem cells as a monolayer on these hydrogels was challenging likely due to weak specificity of the peptide to stem cells or change in mechanical properties of the hydrogels. In this study, we developed thermally expandable hydrogels incorporating fibronectin (FN) with tunable adhesive properties of human mesenchymal stem cells (hMSCs). The effect of FN on adhesion, proliferation, and formation of a confluent layer of hMSCs was first examined. We then investigated the effect of several parameters such as temperature and thickness of hydrogels regulating degree and rate of hydrogel expansion, and transfer time on successful detachment and re-attachment of cell patch to various model target substrates (glass, polymeric nanofibers, and subcutaneous tissue of mouse). Finally, we showed the potential delivery of stem cell patch with being committed to osteogenic or adipogenic lineage.

2. Materials and methods

2.1. Materials

Human plasma fibronectin (FN) and purified anti-FN were purchased from BD Biosciences (Franklin Parks, NJ, USA). A synthetic peptide, GRGDGGGGGY, was custom-ordered from AnyGen (Gwangju, Korea). Anti-laminin was obtained from Abcam (Cambridge, MA, USA). Anti-connexin 43 (CX43) was purchased from Cell Signaling Technology Inc. (Danvers, MA, USA). Hoeschst 33258, Vybrant™ DiD cell-labeling solution and Live/Dead viability/cytotoxicity kits were purchased from Molecular Probes (Eugene, OR, USA). Fluorescein isothiocyanate (FITC), anti-mouse IgG biotin conjugate, Mayer's hematoxylin, peroxidase from horseradish (HRP), hydrogen peroxide (H_2O_2) and fluorescamine were purchased from Sigma–Aldrich (St. Louis, MO, USA). Fetal bovine serum (FBS) was obtained from Wisent (St.-Bruno, QC, Canada), and Dulbecco's modified Eagle's medium including low glucose medium (DMEM), Dulbecco's phosphate buffered saline (PBS), trypsin/EDTA, and penicillin–streptomycin (p/s) were purchased from Gibco BRL (Carlsbad, CA, USA). Rhodamine-phalloidin was purchased from Invitrogen Corp. (Carlsbad, CA, USA). FITC-conjugated streptavidin was obtained from ebioscience (San Diego, CA, USA).

2.2. Preparation of hydrogels containing FN and peptide

Tetronic®-tyramine was synthesized and characterized as described previously [24]. Briefly, terminal hydroxyl groups of Tetronic 1307 (4-arm-polypropylene oxide–polyethyleneoxide, MW. 18,000, BASF, Germany) was conjugated with *p*-nitrophenylchloroformate (PNC) to form Tetronic®-PNC, which was subsequently used to synthesize Tetronic®-tyramine by coupling reaction between Tetronic®-PNC and tyramine. The hydrogels were prepared by previously described methods with minor modifications [24,25]. We prepared two separate solutions of Tetronic®-tyramine with (1) 0.1 wt% of H_2O_2 in PBS and (2) 0.025 mg/ml of HRP in PBS. The solution (2) contained defined concentrations of FN (10, 25, and 50 μg/ml for FN-10, FN-25, and FN-50 hydrogels, respectively) or cell-adhesive RGD-containing peptide (4 mg/ml). The final concentration of Tetronic®-tyramine in all groups was equally adjusted to 7.63 wt%. The two solutions were separately filled within the chamber of the dual-syringe, which were then co-injected into the space between glass plates separated by a Teflon spacer. The crosslinking reaction rapidly occurred within 1–2 min to form hydrogels incorporating FN or peptide. After the *in situ* crosslinking reaction, circular-shaped samples were obtained using a biopsy punch (8-mm diameter, Stiefel®, Verkaufsinnendienst, Germany). The code names and compositions of the hydrogel used in this study are listed in Table 1.

2.3. Characterization of hydrogels

The incorporation of FN within the hydrogels was confirmed using fluorescence-based techniques. FN hydrogels (8 mm in diameter, 0.5 mm in thickness) were immersed in 1 ml of an FITC solution (2 mg/ml in EtOH) at room temperature for 4 h and then continuously washed with EtOH for 2 h and PBS for 6 h. FITC-labeled FN hydrogels were visualized using a fluorescence microscope (Nikon TE-2000, Nikon Corp., Tokyo, Japan). Using NIH Image J medical imaging software (http://rsbweb.nih.gov/ij/, National Institutes of Health, Bethesda, MD, USA), the relative fluorescence units (RFU) of the FN distribution was quantified. The incorporated FN density on hydrogels was determined by a fluorescamine assay. Briefly, hydrogel discs (8 mm in diameter, 0.5 mm thick) were placed in a microtube containing 1 ml PBS solution under orbital shaking (RPM 250, 37°C). At designated time points, the solution was collected and immersed in another 1 ml of fresh PBS solution. The supernatant was collected and subsequently reacted with a fluorescamine solution (100 μg/ml in acetone) for 60 s under vortexing. The fluorescent intensity of the supernatant was analyzed using a spectrofluorometer (Molecular Devices, Sunnyvale, CA, USA) at an excitation and emission wavelength of 390 nm and 475 nm, respectively. A standard curve was prepared with FN solutions (0.05–50 μg/ml). The FN reaction yield was determined using the following equation: (FN reaction yield (%) = (value for the theoretically incorporated FN into the hydrogels − value from experimental FN density on the hydrogels) x 100). The Young's modulus of the FN

Table 1
Composition of FN-hydrogels.

Sample code	Component A (HRP)[a]		Component B (H_2O_2)[b]
	Tetronic®-tyramine Concentration (wt%)	Fibronectin concentration (μg/ml)	Tetronic®-tyramine concentration (wt%)
FN-0	7.6	0	7.6
FN-10	7.6	10	7.6
FN-25	7.6	25	7.6
FN-50	7.6	50	7.6

[a,b]The Final concentration of Tetronic®-tyramine in all blended solution was 7.6 wt%.

hydrogels was calculated using atomic force microscopy (AFM; Asylum Research, Goleta, CA, USA). For measurements, the FN hydrogels (diameter: 8 mm) were attached to a glass slide and placed on a chamber, and then measured using SiN cantilever. The temperature-dependent changes in the size of the FN hydrogels were measured with alternating temperature (37, 25, and 4°C). FN hydrogels (8-mm diameter) were immersed in 1 ml of PBS and sequentially incubated at 37, 25, and 4°C for 30 min. The change in size of the FN hydrogels by temperature was recorded at each time point using a Vernier caliper (Mitutoyo Corp. Kawasaki, Japan). The kinetics of the size change in the FN-50 hydrogels under 4°C was obtained every 1 min up to 10 min and then every 10 min up to 30 min. The relative size of the FN hydrogels under alternating temperature (25 and 4°C) was normalized by the size of the initial FN hydrogel at 37°C.

2.4. Adhesion and proliferation of hMSCs on hydrogels

Human mesenchymal stem cells (hMSCs, Lonza, Basel, Switzerland) were cultured in DMEM supplemented with 15% FBS and 1% p/s antibiotics under standard culture conditions (37°C, 5% CO_2). The hMSCs were seeded onto the hydrogels at a density of 1×10^4 cells/cm^2 and cultured for 12 h. Cells were then fixed in 4% paraformaldehyde and permeabilized with cytoskeletal buffer (pH 6.8, 50 mM NaCl, 150 mM sucrose, 3 mM $MgCl_2$, 50 mM trizma-base, 0.5% Triton X-100). The permeabilized cells were treated with rhodamine-phalloidin (1:100) and Hoechst 33258 (1:5000) to stain for F-actin and nuclei, respectively. The projected cell areas of adherent hMSCs were determined with a fluorescence microscope (TE-2000, Nikon Corp., Tokyo, Japan) using Nikon image software (NIS-Elements AR, Nikon Corp., Tokyo, Japan). In addition, we used other cell types for the study of interactions with hydrogels incorporating RGD peptide; human dermal fibroblasts (hDFB) purchased from Gibco BRL (Carlsbad, CA, USA), cultured in HG-DMEM with 10% FBS and 1% p/s antibiotics, and human umbilical vein endothelial cells (HUVEC), purchased from Lonza Ltd. (Basel, Switzerland) were cultured using EGM-2 Bullet kits. We also incubated pure hydrogels within 20 μg/ml FN solution for 2 h to compare the effect of FN on stem cell adhesion with being presented as immobilized versus physically coated.

Cell proliferation on the hydrogels was evaluated for 72 h with a 4-[3-(4-iodophenyl)-2-(4-nitrophenyl)-2H-5-tetrazolio]-1,3-benzene disulfonate (WST-1) EZ-Cytotox assay kit (ITSBIO, Seoul, Korea). Briefly, cells on hydrogels were replenished at each assay point (12, 24, 36, 48 or 72 h) with a working solution and further incubated for 2 h. The enzymatic activity was then measured at 440 nm using a spectrophotometer. All data was calibrated with an absorbance value calculated using a cell-free hydrogel group and treated with the same working solution.

2.5. Effect of hydrogels and temperature change in transfer stamping of cell patch

hMSCs labeled with a cell-tracker dye (Vybrant™ DiD (red)) were seeded onto the FN-50 hydrogels at a density of 2.5×10^4 cell/cm^2 at 37°C for 24 h to allow the cells to form a confluent cell layer. The confluent hMSCs on the hydrogels at 37°C were gently placed over the glass and the temperature was lowered to 25 or 4°C while incubation was maintained under the reduced temperature from 5 to 30 min. The hydrogel was then peeled off from the target leaving cell patch, which was fixed with 4% paraformaldehyde and analyzed using Image Station (4000 MM, Eastman Kodak Company, Rochester, NY, USA). Using Image J software, the relative fluorescence units (RFU) from the fluorescently-labeled hMSC patch on glass was quantified. In order to confirm the viability of the transferred hMSC patch, a Live/Dead viability/cytotoxicity kit was used immediately after the process, wherein a solution mixed with calcein AM (1:1000, green for living cells) and ethidium homodimer-1 (1:500, red for damaged cells) was exposed to the transferred hMSC patch for 30 min. The hMSC patch was then imaged using a fluorescence microscope in which the images were captured ($n = 5$ per sample, triplicate), and percentage of live cells over total number of cells was calculated by using Nikon image software. Quantification of transferred cells was also carried out by using Quanti-iT™ PicoGreen® dsDNA assay kit according to manufacturer's procedure.

2.6. Immunofluorescence staining of the hMSC patch

The structure of the hMSC patch was analyzed by immunofluorescence staining for CX43, F-actin, FN, and laminin. After the transfer process, the hMSC patch was fixed in 4% paraformaldehyde and then permeabilized with cytoskeleton buffer. The permeabilized samples were treated with blocking buffer for 1 h, and then sequentially incubated with primary antibodies (anti-FN (1:100), anti-laminin (1:100) and anti-CX43 (1:50)) for 1 h and anti-IgG biotin conjugate (1:100), and FITC-conjugated streptavidin (1:100) for 1 h. Cell nuclei and F-actin were stained with Hoechst 33258 and rhodamine-phalloidin, respectively.

2.7. Versatile transfer stamping of hMSC patch

Fibrous meshes and films of poly(L-lactide) were prepared from electrospinning and solvent evaporation method, respectively. The hMSC patch was then transferred onto them by changing the temperature from 37°C to 4°C for 10 min, which was stained with Mayer's hematoxylin for 10 min, and observed by scanning electron microscopy (SEM) and phase contrast microscopy. The transferred hMSC cell layer on subcutaneous tissue was monitored by pre-labeled hMSCs. 7-week-old, male Balb/C mice were anesthetized with zoletil (50 μg/g body weight) and the dorsal skin was cut in a "U" shape and the skin was immediately flipped onto the mice's back and the hMSC patch cultured on the hydrogels (circle, diameter: 8 mm) placed on the dorsal skin. Cool (4°C) saline was periodically dropped onto the hydrogels for 5, 10, 15, and 30 min, and then the hydrogels were peeled off the skin. After the transfer process, the incision was closed with 5-0 nylon sutures. All animals were treated in accordance with experimental procedures approved by Hanyang University (HY-IACUC-12-073). Mice were then anesthetized and the fluorescence intensity from the pre-labeled hMSC patch on the subcutaneous tissue was observed using Image Station. After 3 days, the mice were euthanized and a 15 × 15 mm section of the dorsal skin was removed. The collected skin tissue was fixed with 4% para-formaldehyde and embedded with paraffin. After the process, 4-μm thick sections were cut with a microtome and visualized for fluorescent-labeled hMSC patch in the histological section by using fluorescence microscopy. For the staining, the retrieved specimen were deparaffinized in xylene, serially hydrated with graded EtOH (100-70%), and treated with Harris hematoxylin. Slides were then mounted with mounting medium, which was observed by using an optical microscopy.

2.8. Transfer stamping of differentiated hMSC patches

The hMSCs were cultured on FN hydrogels to confluence. After one day, the media was replenished with two types of differentiation media; 1) osteogenic differentiation media including ascorbic acid, glycerol-2-phosphate, and dexamethasone, 2) adipogenic differentiation media including 3-isobutyl-1-methylxanthine (IBMX), human insulin, indomethacin and dexamethasone. The hMSCs cultured on FN hydrogels were maintained in specific differentiation media for 7 days, which were transferred to a target glass at 4°C for 15 min. Differentiation of hMSCs was confirmed using an alkaline phosphatase (ALP) kit and Oil Red O staining for osteogenic and adipogenic differentiation, respectively. The hMSCs on FN hydrogels and those transferred to glass were also counterstained with hematoxylin. The hMSCs cultured on FN-50 hydrogels for 7 days under growth media were used as the control group.

2.9. Statistical analysis

All quantitative results were obtained from triplicate samples. Data are expressed as mean ± standard deviation and were analyzed using SPSS 18.0 software (SPSS Inc., Chicago, IL, USA). Statistical analysis was performed using ANOVA and the Tukey HSD test. P values <0.05 were considered to be statistically significant.

3. Results and discussion

Fig. 1 illustrates the overall process of transfer stamping of hMSC patch to the target using thermally expandable hydrogels. FN is covalently incorporated into the hydrogel via one-step crosslinking reaction with the synthesized Tetronic®-tyramine polymer. Incorporation of biomolecules into hydrogel through bulk modification exploited in our study has been used for many years to modulate cell adhesion [26]. Among used biomolecules, peptides including RGD (Arg-Gly-Asp) sequence have been popular although there are several factors to be considered for specific approaches such as structure (linear, cyclic, looped and constrained), varied specificity, spacer length, and sequence arrangement [27–29]. On the other hand, ECM proteins such as FN have also been widely used for the same strategy by presenting numerous synergistic active peptide fragments such as RGD and PHSRN (Pro-His-Ser-Arg-Asn) [30,31]. hMSCs were adherent to the hydrogels incorporated with FN and formed a confluent layer, which was then easily and rapidly transferrable to desired targets (including glass, polymeric nanofibers, and subcutaneous tissue, etc.) upon temperature change from 37°C to lower one.

3.1. Preparation and characterization of FN-hydrogels

The *in situ* incorporation of FN within the hydrogel was first investigated. The relative fluorescence intensity of hydrogels crosslinked with FITC-FN linearly increased with an increase in input concentration (Fig. 2a–c). It was 12.9 times greater for FN-50 hydrogels than that of FN-0, with the reaction yield of 81.2 ± 17.9% and 66.0 ± 10.7% for the FN-10 and FN-50 hydrogels, respectively. In addition, the un-reacted residual FN was detected for over 48 h with no further release. These results indicate that the reaction

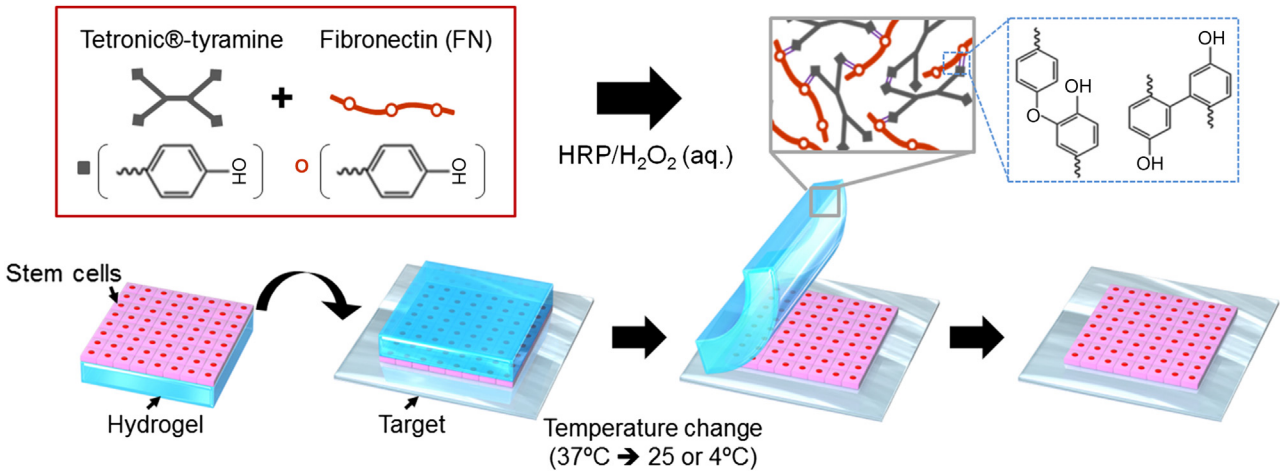

Fig. 1. Schematic illustration of *in situ* incorporation of FN into thermally expandable hydrogels and transfer stamping of a hMSC patch cultured on the hydrogels to a target substrate. Separate solutions of Tetronic®-tyramine and FN are *in situ* crosslinked within few minutes in the presence of HRP and H_2O_2 as a catalyst by using dual syringe. hMSCs are attached to form a monolayer on the surface of hydrogel (thickness can be varied from 0.5 to 1.5 mm for the test). hMSCs cultured on the hydrogel are contacted to the target substrate (glass, nanofibers, or subcutaneous skin) under reduced temperature, and removal of the hydrogel leaves completely transferred hMSC patch stamped on the target surface.

between phenol groups in Tetronic®-tyramine and a number of tyrosine residues in FN (approximately 4.3% out of 2176 amino acids) was successfully carried out to form carbon–carbon and carbon–oxygen bonds by oxidative reactions as previously described [21–25,32]. Functionalized synthetic hydrogels have been prepared by various crosslinking chemistries including free-radical polymerization, Michael-type addition, and a maleimide-based reaction, but, our results suggest that enzyme-mediated crosslinking appears to be a simple and efficient approach to incorporate bioactive molecules within hydrogels [33,34]. The

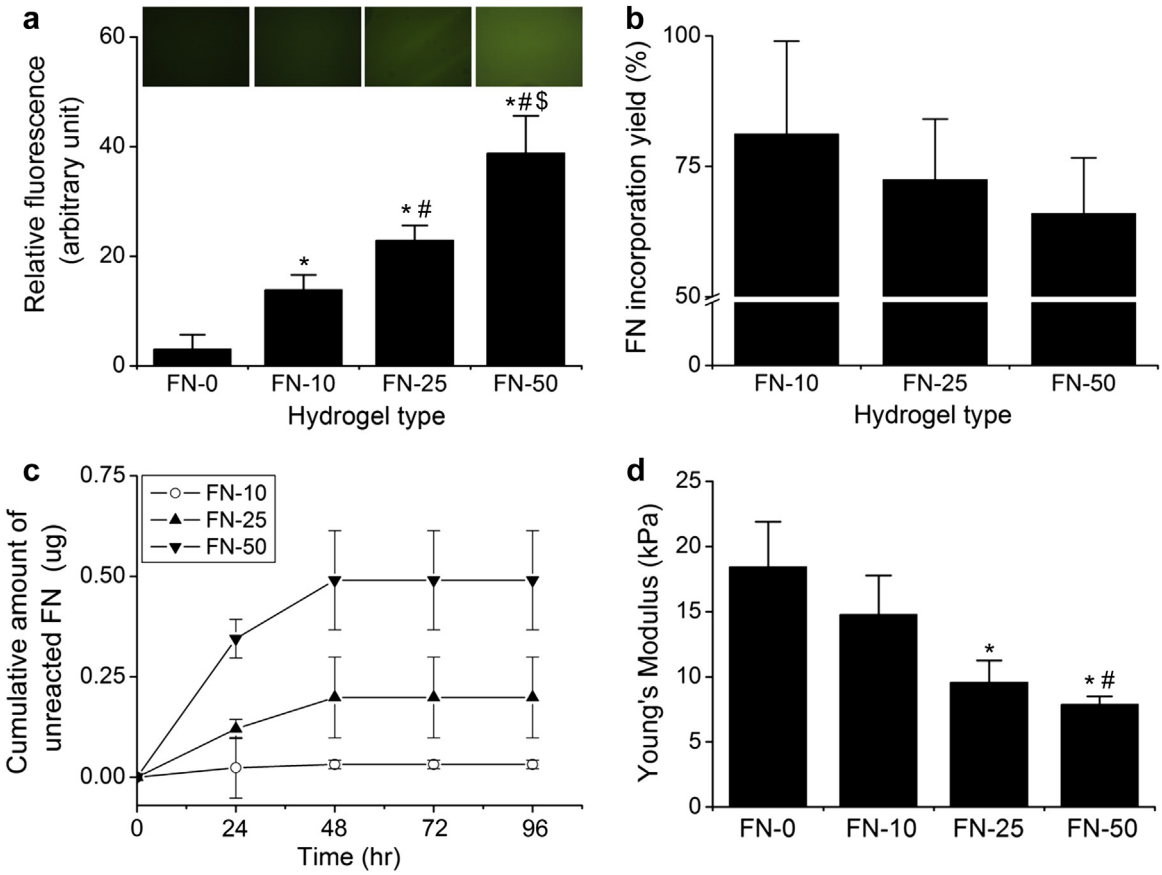

Fig. 2. Characteristics of FN hydrogels. (a) The visualized images of the crosslinked hydrogels reacted with various concentrations of FITC-tagged FN (0, 10, 25, and 50 μg/ml) and relative fluorescence corresponding concentrations. (b) The incorporation yield of FN into the hydrogels where the un-reacted amount of FN was measured and the amount of FN within the hydrogel was then back-calculated. (c) The cumulative amount of un-reacted FN from FN-hydrogels released over 96 h. (d) The Young's modulus of FN-hydrogels measured by AFM. "*", "#" and "$" represent statistical differences as compared to FN-0, FN-10 and FN-25, respectively ($p < 0.05$).

reaction yield decreased as a function of the added amount of FN, which may be attributed to the presence of a fixed number of Tetronic®-tyramine available for reaction with FN and the potential self-polymerization of FN at higher concentrations. Similar to the reaction yield, FN hydrogel Young's modulus (or 'stiffness' as described in biology; measured in Pascal, Pa) decreased as the FN content increased from 18.4 ± 3.5 kPa to 9.6 ± 1.7 kPa for FN-0 and FN-25 hydrogels, respectively. As shown in Fig. 2d, the lower Young's modulus may be attributable to the decrease in the overall number of crosslinks between the Tetronic®-tyramine macromers and an increase in the reactions with FN.

We then characterized thermo-responsive properties of the resultant hydrogels. As shown in Fig. 3, the FN hydrogels exhibited a serial increase in size with response to the reduction in temperature from 37°C to 25°C and 4°C, which underwent a reversible increase/decrease cycle over four iterations between these temperatures. The maximal increase in hydrogel size at 4°C was slightly less when the hydrogel was crosslinked with FN, however, no statistical difference was observed (1.20 ± 0.02, 1.17 ± 0.01, and 1.16 ± 0.02 for FN-0, FN-10, and FN-50 hydrogels, respectively). Tetronic®-based polymers exhibit a transition from a "gel" to a "sol" phase due to enhanced hydrophilic interactions between Poly(-ethylene oxide) (PEO) segments of the polymer with decreasing temperature [35,36]. We also previously demonstrated that the hydrogel prepared from Tetronic®-tyramine resulted in increased hydration by dominant hydrophilicity of PEO at 4°C compared to 37°C [23]. The slight drop in overall hydrogel expansion with FN incorporation may be ascribed to the interference of FN with these strong interactions between polymer segments. Notably, the relative size of the FN-50 hydrogels rapidly increased and reached a plateau within 10 min when the temperature was cooled from 37°C to 25°C and 4°C. Rapid expansion of hydrogels leading to rapid cleavage in receptor/ligand binding between stem cells and FN is essential to transfer stamp the stem cell patch to target substrates. Otherwise, intact cell–cell junctions would be damaged during the transfer process.

3.2. Adhesion and proliferation of hMSCs on FN-hydrogels

The effect of FN hydrogels on adhesion and proliferation of hMSCs were then investigated. As shown in Fig. 4a and b, hMSCs were barely adhered and aggregated to the hydrogel without FN while attached well to FN-hydrogel and their morphology was remarkably influenced by FN concentration. The F-actin network formation indicative of mature cell spreading was minimally observed in hMSCs cultured on hydrogels with lower concentrations of FN-10 and -25 hydrogels, but, mature stress fiber was clearly visible on FN-50 hydrogels. Over 70% of the quantitatively-measured area of adherent hMSCs on FN-10 hydrogels was limited to less than 3000 μm^2, whereas the distribution was shifted to a higher region (6000–15000 μm^2) for hMSCs cultured on FN-50 hydrogels. When hMSCs were cultured on FN-hydrogels for 3 days, the cell number significantly increased with the FN concentration (Fig. 4c and d). The absorbance from hMSCs cultured on the FN-50 hydrogels was 0.15 ± 0.04 at 24 h, which significantly increased to 0.24 ± 0.01 at 48 h, however, the proliferation of hMSCs on other types of hydrogels was limited. The proliferation on the FN-50 hydrogels also appeared to stop after 48 h, but it was related to complete confluence of hMSCs on the hydrogel.

We then tested the specificity of FN-hydrogels on stem cell adhesion. As shown in Fig. 5a, the morphology hMSCs was retained circular after 12 h of adhesion, with no evidence of healthy spreading on hydrogels without incorporation of FN. Additionally, hMSCs did not attach well to the hydrogels coated with FN despite the use of FN with high concentration, implying that covalent immobilization of FN within the hydrogel is required for modulation of stem cell adhesion. These results also re-confirmed the non-fouling characteristic of our hydrogels (probably minimizing protein adsorption). We also used hydrogels containing RGD peptide and verified their interactions with hMSCs. As shown in Fig. 5b, unlike those on FN-hydrogels, hMSCs poorly adhered on such hydrogels after 12 h and detached from them for the next few days. We increased the peptide concentration and seeding density, however, none of our trials gave us positive results (data not shown). In contrast, the same type of hydrogels containing RGD peptides successfully supported complete monolayer formation of hDFB and HUVEC at the same seeding density experimented with hMSCs.

Our results here are quite unexpected since the cell-interactive peptide sequence (RGD) used in our study along with FN have been widely utilized to enhance interactions on stem cell/biomaterial interface [37–39]. Previous works demonstrated that the adhesive layer provided from these cell-interactive peptide helped stem cells effectively adhere and spread on a biomaterials in some way or another. However, it has also been increasingly evident that the complex inherent properties of engineered microenvironment

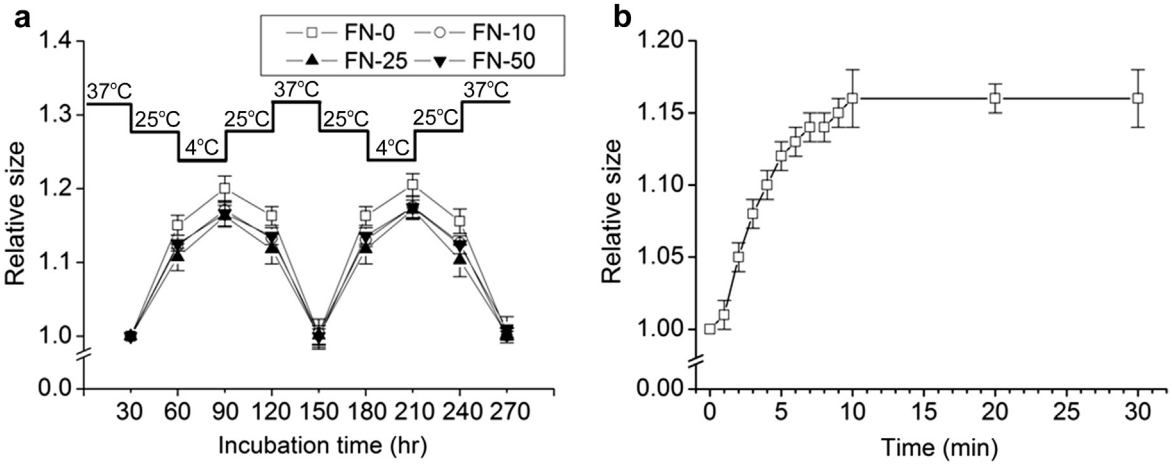

Fig. 3. (a) The reversible size change of FN hydrogels in PBS in response to different temperatures (37, 25, and 4°C). At each temperature, the hydrogel was incubated for 30 min and the size of the hydrogel was then measured and compared to that at 37°C. (b) The expansion kinetics of FN-hydrogels over 30 min when the temperature was reduced from 37°C to 4°C.

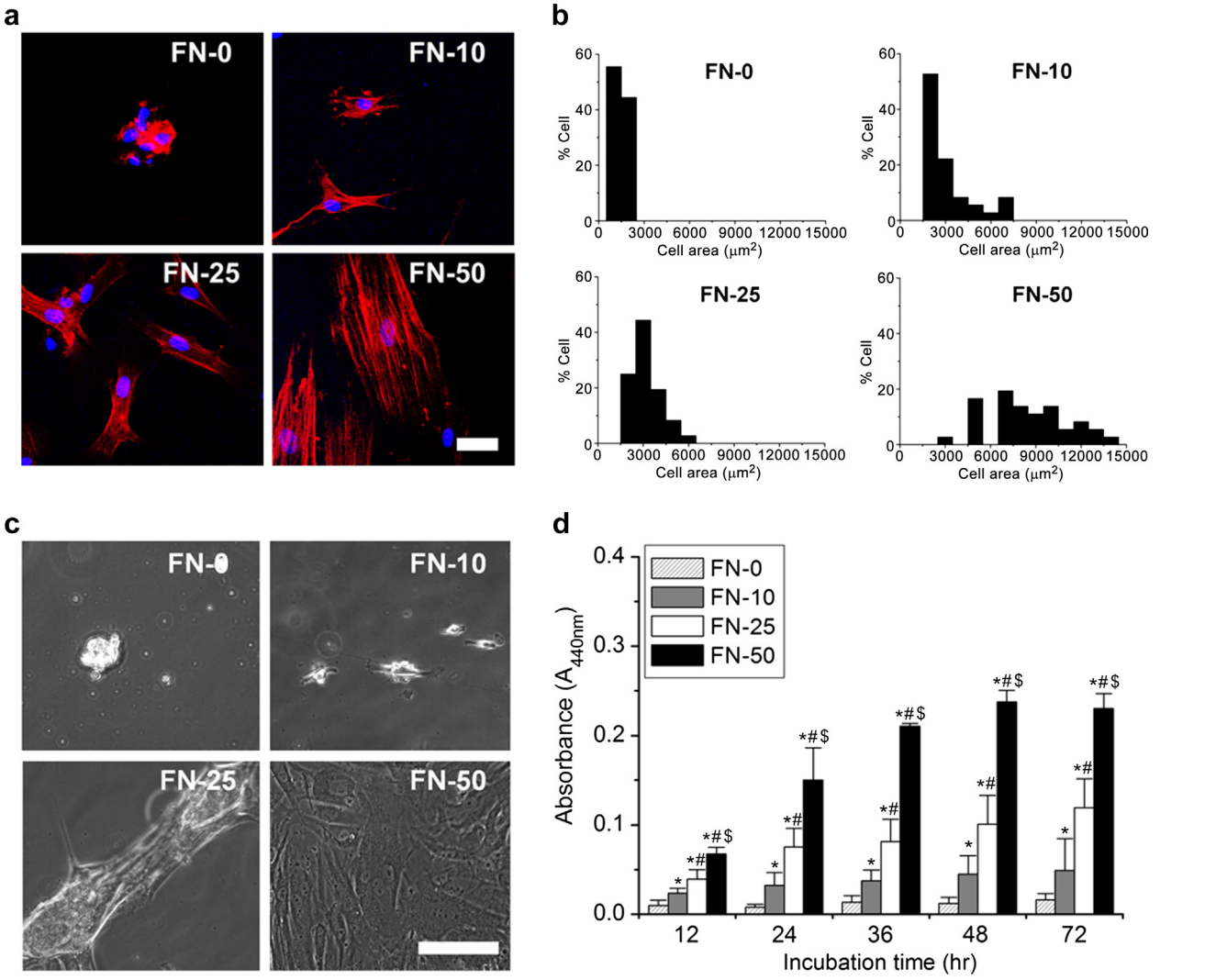

Fig. 4. The effect of FN concentrations incorporated into hydrogels on adhesion and proliferation of hMSCs. (a) Cytoskeletal structure and morphology and (b) distribution of the adherent hMSC area on FN hydrogels corresponding to the F-actin stained results (n > 50). (c) Phase contrast images of hMSCs cultured on FN hydrogels for 48 h and (d) proliferation of hMSCs cultured on FN hydrogels for 72 h under growth media. Scale bars indicate 50 μm "*", "#" and "$" represent statistical differences as compared to FN-0, FN-10 and FN-25, respectively at each time point ($p < 0.05$).

such as stiffness, cell-binding affinity, molecular flexibility of cell interactive domains, and surface topography could also play key factors to regulate stem cell behaviors [40]. For example, it has been reported that materials with a low mechanical modulus is often difficult to support robust stem cell adhesion despite the presence of sufficient chemical signals; hMSCs cultured on relatively soft hydrogels (~10 kPa) with RGD peptide were not well spread, with cell spreading increasing with hydrogel modulus [1,2,41,42]. In addition, the process for stem cells to sense inherent properties of contacting materials seems to be highly complex such that aforementioned factors are independently or synergistically correlated to each other; density and length of linker to which proteins are covalently tethered, and protein dynamics controlled by micro/nano scaled anchoring points on the surface of hydrogels may exist but the exert degree of influence on stem cell function versus stiffness is still unresolved [1,43]. Our system is even more complicated than these previous hydrogels in that proteins are *in situ* crosslinked within 3-dimensional network, in which entanglement of Tetronic® polymer chains may additionally suppress flexible dynamic presentation of cell-adhesive domains toward the surface of hydrogels. The underlying mechanism is an interesting subject for further investigation. Nonetheless, presentation of FN in our hydrogel was able to support full spreading of hMSCs under a relatively soft mechanical environment, which was the critical progress for transfer stamping of monolayer of hMSCs.

3.3. Temperature-dependent transfer stamping of hMSCs patch

The thermo-responsive *in vitro* detachment and re-attachment of hMSC patch was then examined. Overall, the relative diameter change after 30 min of incubation was affected by hydrogel thickness; a 0.5 mm hydrogel displayed the highest expansion, which was remarkably significant in the transition to 4°C (Fig. 6a and b). These aspects may be explained by faster water penetration into the thinner hydrogels under a fixed incubation time, and thus may facilitate an increase in hydrogel diameter. In addition, the fluorescence intensity of the transferred hMSC patch on the glass was concomitantly influenced by these two factors. As shown in Fig. 6c and d, the entire hMSC patch was transferred and visible on glass when the process was performed with a 0.5 mm hydrogel at 4°C while only the periphery of the hMSC patch was transferred with the 1.5 mm hydrogels at 25°C. Furthermore, the reduced

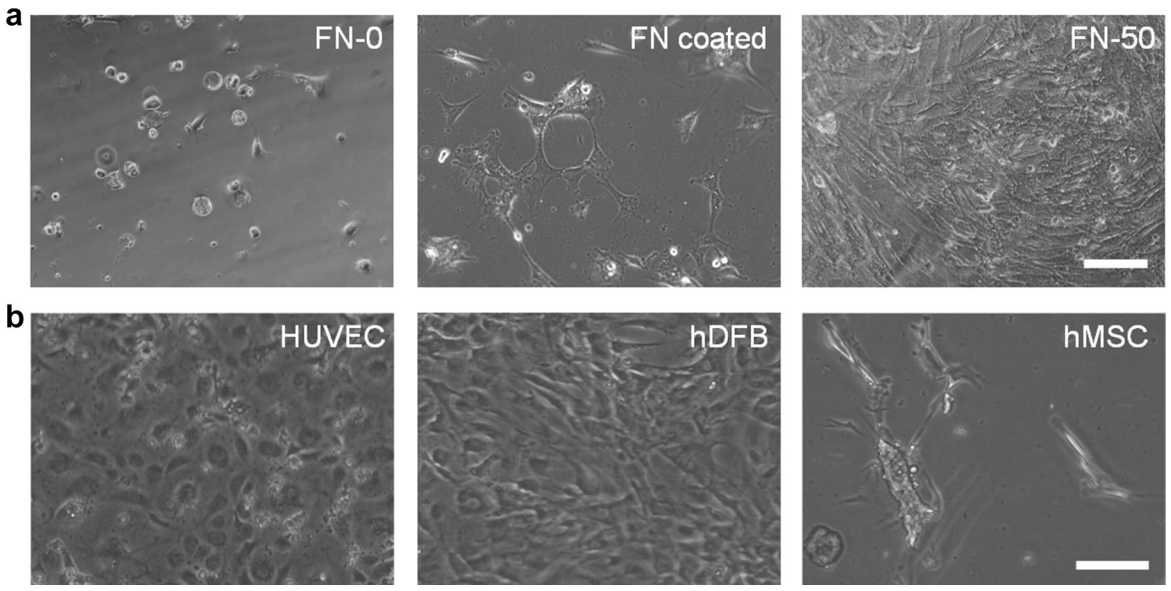

Fig. 5. (a) The morphology of hMSCs attached on hydrogels prepared by various conditions. FN-0 represents the hydrogel without FN incorporation, FN coated represents the hydrogels crosslinked without FN, but were then coated with FN solution (20 μg/ml) for 2 h before cell seeding, and FN-50 represents the hydrogel *in situ* crosslinked with FN (50 μg/ml), (b) The effect of RGD-containing peptide in hydrogel on adhesion of hDFB, HUVECs, and hMSCs. Scale bars indicate 200 μm.

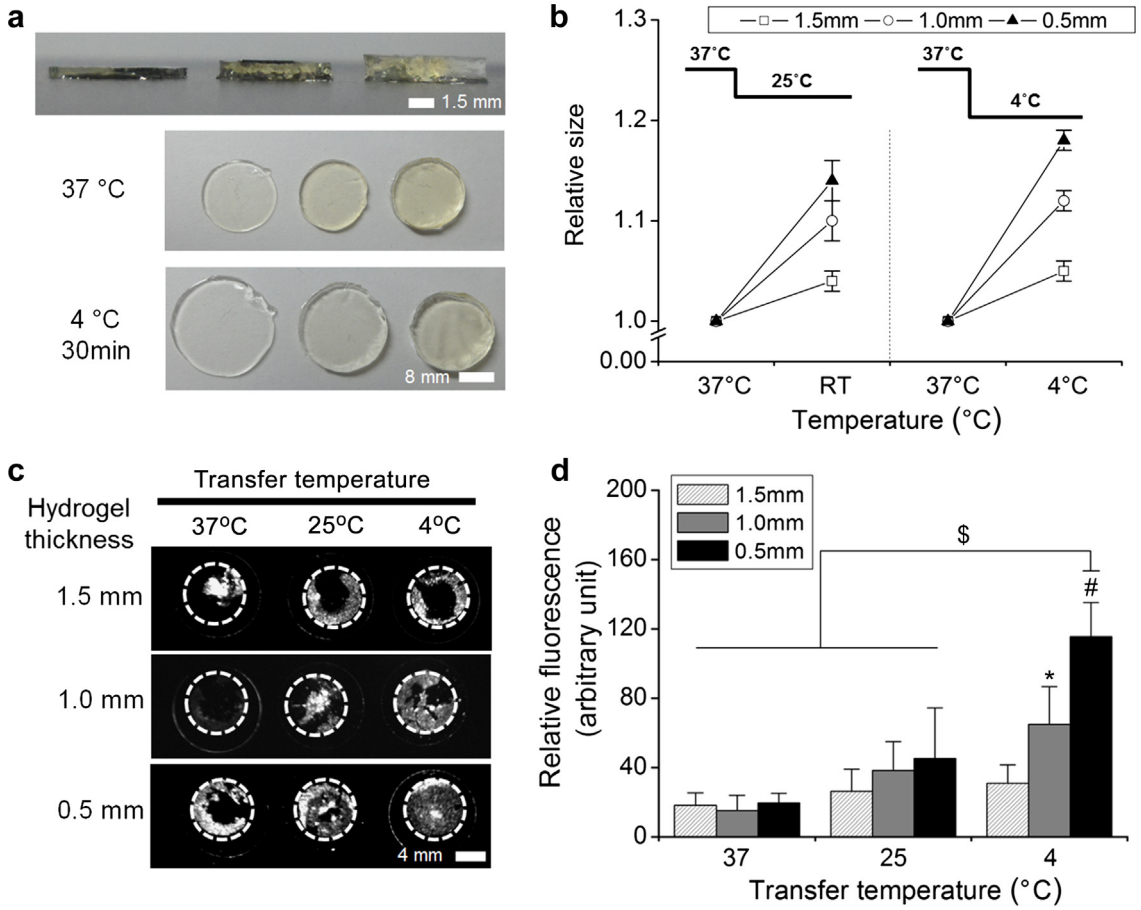

Fig. 6. (a) The side-view macroscopic images of FN-50 hydrogels from at 37°C and the top-view under 37°C (top) and 4°C (bottom) after 30 min of incubation. (b) The relative size of FN-50 hydrogels in PBS in response to temperature change from 37°C to 25 and 4°C for hydrogels with thicknesses of 1.5, 1.0, and 0.5 mm. (c) Representative images of the transferred fluorescence-labeled hMSC patch on glass under different conditions (thickness of hydrogels, temperature) observed by an image station and (d) the quantification of their relative intensity. "*" and "#" represent statistical differences as compared to thickness of hydrogels with 1.5 mm and 1.0 mm, respectively. "$" indicates significance as compared to the transfer temperature at 37°C and 25°C ($p < 0.05$). Scale bars indicate 4 mm.

temperature serves as a dominant driving force to detach the hMSC patch as there was very limited fluorescence at 25°C and 37°C (45.29 ± 29.20, and 19.69 ± 5.45, respectively) compared to that at 4°C (115.56 ± 19.74). We then used 0.5 mm FN-50 hydrogels at a fixed temperature of 4°C, and the time required for complete detachment and re-attachment of the hMSC patch and its effect on cell viability were examined. Fig. 7a demonstrates that the fluorescence intensity reached the same level when a transfer time greater than 15 min was applied, which was significantly greater than that from 5 to 10 min, in which only minimal number of cells were successfully detached and re-attached. The Live/Dead staining revealed that the transfer time influenced cell viability. As shown in Fig. 7b, the hMSCs were completely viable for 15 and 30 min groups while a large number of cells were detected as dead when the transfer time was less than those. Measurement of number of cells that were transferred to the glass showed 1.18×10^4 and 1.21×10^4 cells/cm^2 for 15 and 30 min of transfer time, respectively, which were close to the number of cells originally present on the hydrogel before transfer process, indicating that complete stamping of hMSCs from the hydrogel to the glass was successful (Fig. 7c). Quantification of images from live/dead assay revealed that almost 100% cells over the total number of stamped cells were alive under the condition of both 15 and 30 min of transfer, while the relative viability of transferred cells reduced to approximately 76.26 ± 6.39 and 30.33 ± 18.77%, for 10 and 5 min, respectively (Fig. 7d). Collectively, these results suggest two important features: (1) incubation of hMSCs under reduced temperature for 30 min has no detrimental effect of cell condition, and (2) cells may be mechanically damaged if the time for detachment and re-attachment is not sufficiently provided.

This aforementioned phenomenon can also be deduced with the size expansion kinetics of FN-hydrogels. Unlike the PNIPAAm-based approach, where the polymer chains become hydrated and extended in nano-scale range upon temperature-mediated transition thereby allowing cell-patch detachment, the present hydrogels undergo macroscopic rapid expansion under a reduced temperature. As shown in Fig. 3b, FN-50 hydrogels showed maximal size change within 10 min at 4°C [23]. It is anticipated that the complete transfer of hMSCs only occurs if sufficient time permits re-attachment of the hMSC patch onto the glass. Peeling-off of the incompletely expanded hydrogels appears to forcibly pull out cells and, therefore, may cause significant physical damage to cells, leading to significant cell death. Despite the potential detrimental effect by our proposed process, the temperature-induced expansion of the hydrogel intuitively offers rapid harvest and transfer of the cell patches. Conventionally, the time required for harvesting a cell patch varies from 30 min to several hours and attempts have been made to rapidly detach cell layers using a synthesized

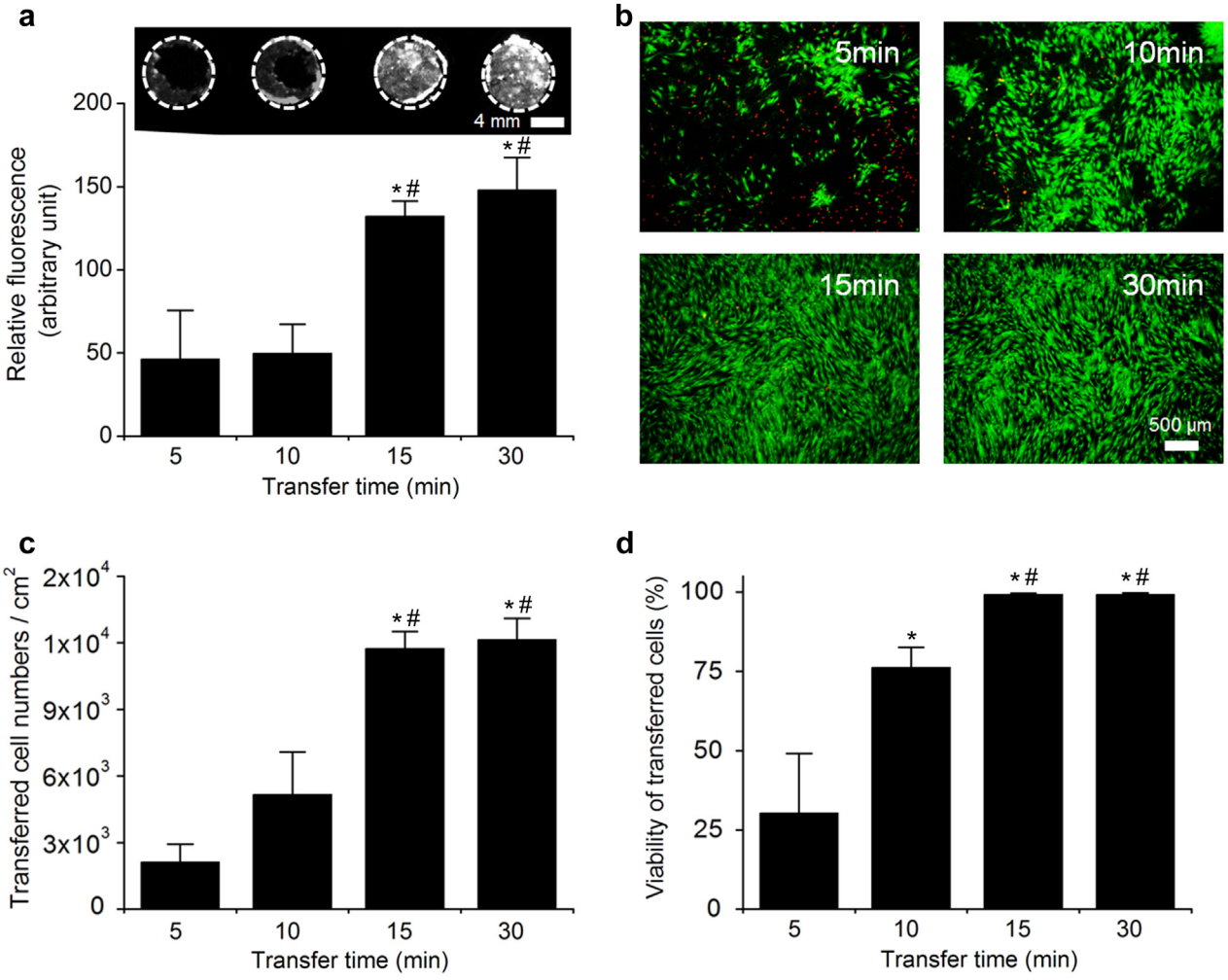

Fig. 7. (a) Representative images of the fluorescence-labeled hMSC patch stamped on glass with different transfer times; 5, 10, 15, and 30 min at 4°C and the quantification of the relative fluorescence intensity. (b) Representative Live/Dead assay images of hMSCs after transfer stamping. (c) The quantification of the number of cells stamped on the glass. (d) The viability of stamped cells according to the different transfer time conditions. "*" and "#" indicate statistical significance in comparison with the condition for transfer time for 5 and 10 min, respectively ($p < 005$). Scale bars indicate 4 mm for (a) and 500 μm for (b).

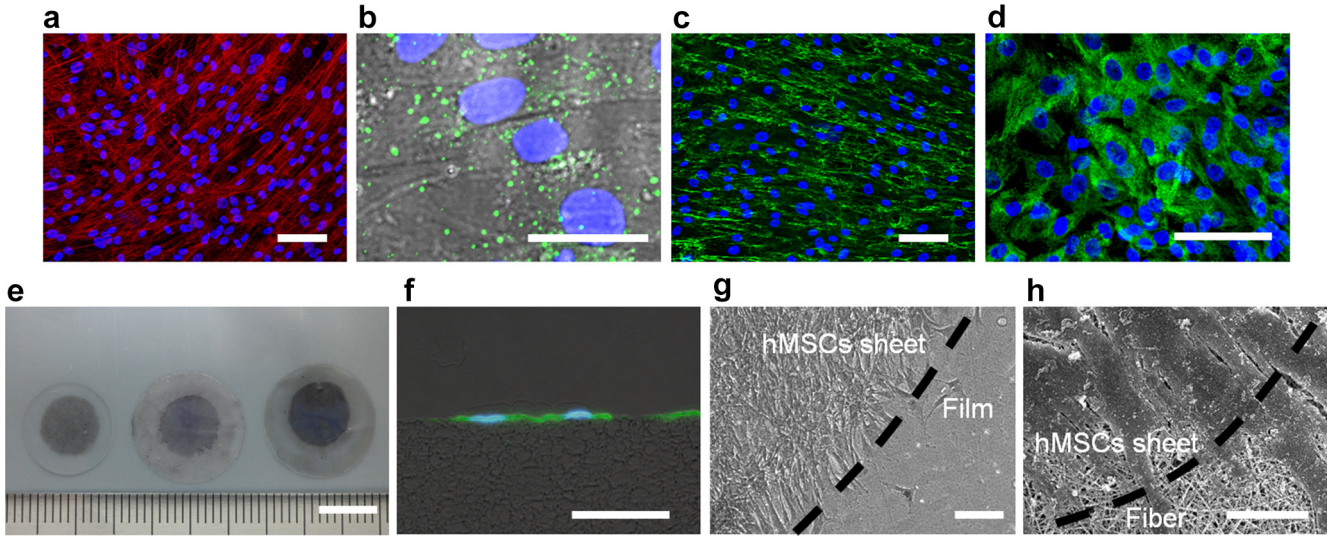

Fig. 8. Representative images of hMSC patches after transfer printing by fluorescence staining for (a) F-actin, (b) connexin 43 (CX43), (c) FN, and (d) laminin. (e) Macroscopic images of the stamped hMSC patch on different substrates (glass, fiber, and film) that were stained by hematoxylin. (f) Cross-sectional images of transferred hMSCs on fibers that were pre-labeled with green fluorescence dye. The periphery of the transferred hMSC patch by phase contrast for (g) film and SEM for (h) electrospun fiber. Scale bars indicate 500 μm for (a, f, g) and 50 μm for (b, h) and 200 μm for (c,d), 8 mm for (e). (For interpretation of the references to color in this figure legend, the reader is referred to the web version of this article.)

polymer brush, spin-coating, and modified chemistry [44–46]. Although these techniques were successful for facilitating detachment of the cell layer from the surface, the developed FN-hydrogels must benefit from simplicity and rapid harvest of the transferrable hMSC patch in an effective manner.

3.4. Characterization of the hMSCs patch

Preservation of the cell cytoskeletal structure and ECM assembly of hMSCs on the target were confirmed after the transfer process. The transferred hMSCs exhibited a highly-crosslinked actin and FN network with no indication of destruction in the cell–cell adhesion. Additional ECM protein, laminin was highly expressed and retained on the stamped hMSCs. In particular, a gap junction protein (CX43) implicated in the survival of stem cells was also clearly observed and localized within the cytoplasm on the transferred hMSCs (Fig. 8a–d). These results suggest that the transferred hMSC patch retained highly organized cell–cell and cell-ECM interactions upon harvest. The study with other target substrates including electrospun fibers, solvent-cased films, and subcutaneous tissue that are

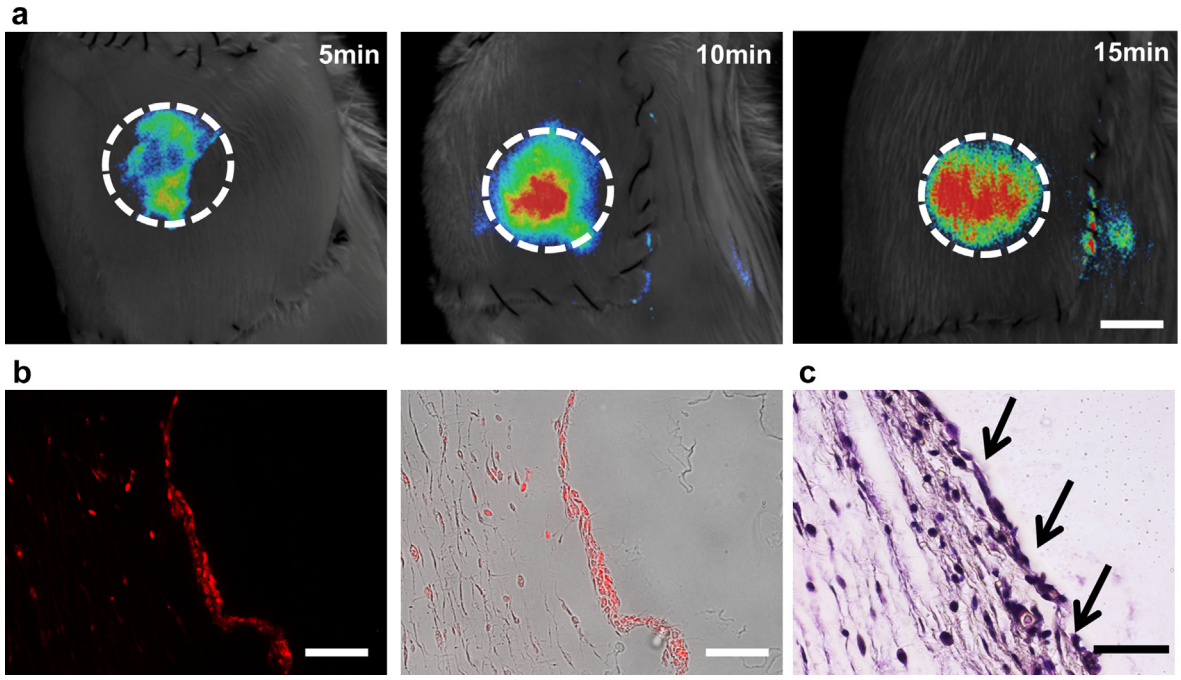

Fig. 9. (a) Direct transplantation of hMSC patch using transfer stamping on subcutaneous skin tissue with transfer times of 5, 10, and 15min. For visualization, hMSCs were pre-labeled with a cell-tracker dye (Vybrant™ DiD) before being cultured on the FN-50 hydrogels. (b) Fluorescent images of transplanted hMSC patch in the histological section. (c) Histological analysis of the transplanted hMSC patch using hematoxylin. Arrows represent the transferred hMSC patch. Scale bars indicate 8 mm for (a) and 50 μm for (b) and (c).

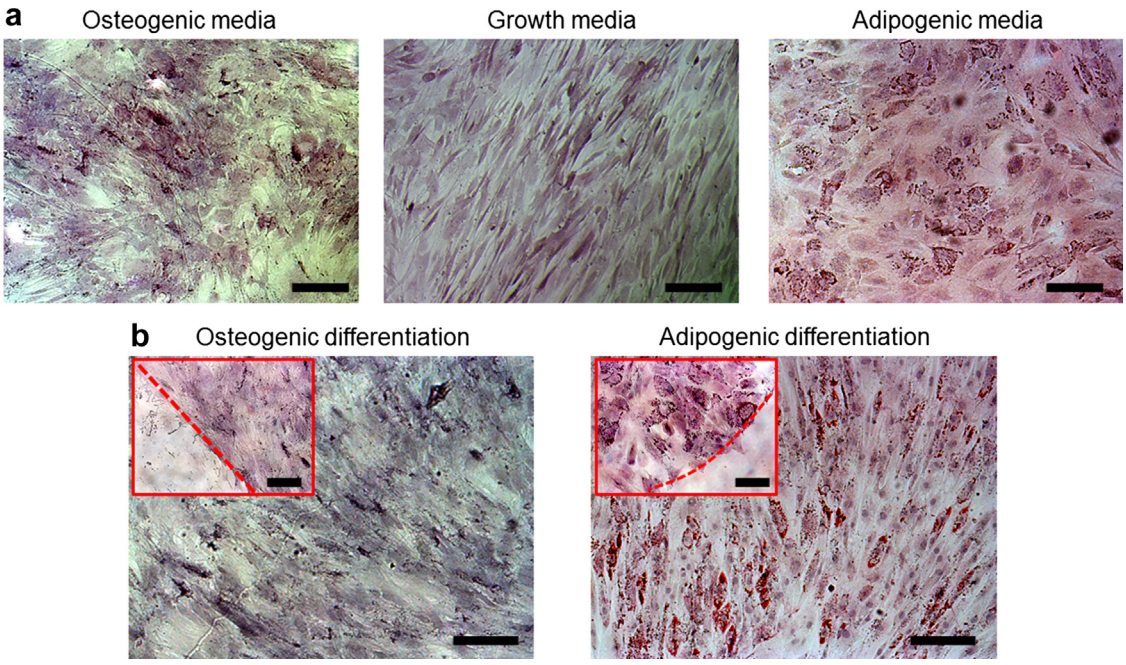

Fig. 10. (a) The representative images of the hMSCs on FN hydrogels under specific media conditions for 7 days. (b) Transferred differentiated hMSCs patch on glass stained with ALP and Oil Red O for osteogenic and adipogenic differentiation, respectively; transferred hMSCs patch on glass were also counterstained with hematoxylin. Scale bars indicate 200 μm. (For interpretation of the references to color in this figure legend, the reader is referred to the web version of this article.)

commonly used in tissue engineering demonstrated that hMSC patches were completely transferred to them with circular shape (Fig. 8e–h).

Most importantly, the transfer of the hMSC patch harvested from FN-50 hydrogels to subcutaneous tissue was facilitated within 15 min (Fig. 9a) The intensity of fluorescently-labeled hMSC patch remarkably increased with contact time from 5 to 15 min. Native tissue is rich in numerous ECM proteins that must be sufficient to ensure strong binding to the hMSC patch within short time. The pre-labeled hMSCs was then visualized by standard preparation for histology, where thin layer of transplanted hMSC patch was clearly shown as presented in Fig. 9b. Hematoxylin staining revealed that the transferred stem cell layer was localized within the injured region after the surgery (Fig. 9c). The most common method to harvest cell patch based on PNIPAAm-grafted culture dishes requires two step processes, in which cell monolayer is transferred to hydrophilically-modified poly(vinylidene fluoride) (PVDF) membrane from culture dish, and subsequently transplanted to the target tissue from PVDF membrane [47,48]. It has been reported that the time required for successful engraftment of cell patch depends on cell types and amount of ECM produced with 5–10 min for minimal compromise in cell patch integrity [49]. With our results, it should be noted that successful engraftment of stem cell patch to subcutaneous tissue can be achieved within 15 min from cell-adhesive hydrogel surface by mechanical expansion.

To demonstrate feasibility of whether hMSC patch differentiated into a desired lineage could be transferred, hMSCs cultured on FN-50 hydrogels were directed into adipogenic or osteogenic lineages using its corresponding media. ALP and Oil Red O staining confirmed the differentiation of the hMSC monolayer cultured on FN-50 hydrogels into osteogenic and adipogenic lineages, respectively (Fig. 10). These results suggest that FN-50 hydrogels are an excellent substrate to control the lineage-dependent culture of the hMSC monolayer despite a relatively low stiffness. The transfer of the hMSC patch differentiated into two distinct lineages was also successfully transferred to the target substrate under the aforementioned conditions. With advances in cell patch technology, more efforts have been made to deliver stem cell patch with appropriate stemness and desirable differentiated stage. For example, treatment of plasmid of bone morphogenetic protein 2 on stem cell patch demonstrated improved bone formation and l-ascorbate 2-phosphate (A2-P) was used to facilitate patch formation of adipose-derived stem cells (ASCs) while maintaining osteogenic and adipogenic differentiation capabilities [50,51]. Our proof-of-concept results may be further exploited to harvest stem cells patch with modulated multilineage. Collectively, our data revealed that a functionalized thermo-responsive hydrogel can be easily used to rapidly harvest a transferrable stem cell patch based on under a one-step process, which may extend the cell patch technology to more practical tissue regeneration applications.

4. Conclusions

In summary, thermally expandable hydrogels were prepared with FN as a cell-interactive cue, which was used to “effectively and rapidly” harvest and transfer hMSC patches. The resultant FN-hydrogels are soft materials where the presentation of cell-adhesive signals and mechanical properties can be easily tuned. The hMSC layer with a size identical to the precisely-controlled shape of the hydrogels can be cultured and transferred to a variety of targets including polymer film, non-woven mesh, and subcutaneous tissue within less than 15 min under a reduced temperature. In addition, the hMSC monolayer on FN-50 hydrogels can be differentiated into a particular linage, which can also be transferred to a target. Collectively, the hydrogels with FN improve and complement current cell patch technology with two remarkable advances: (1) promoted adhesion and spreading of hMSCs to allow for formation of a complete monolayer that can then be rapidly transferred to a target, and (2) support of the differentiation of monolayered hMSCs into various lineages for several days, enabling easy transfer to a target. Further work may involve transplantation of a differentiated hMSC layer using our approach

to prove its therapeutic effects and improve transfer conditions for more effective clinical applications.

Acknowledgments

This work was supported by the National Research Foundation of Korea (NRF) grant funded by the Korea government (MSIP) (No. 2013R1A2A2A03067809) and by the Korea Health Technology R&D Project, Ministry of Health & Welfare, Republic of Korea (A121044).

References

[1] Trappmann B, Gautrot JE, Connelly JT, Strange DG, Li Y, Oyen ML, et al. Extracellular-matrix tethering regulates stem-cell fate. Nat Mater 2012;11:642–9.
[2] Dellatore SM, Garcia AS, Miller WM. Mimicking stem cell niches to increase stem cell expansion. Curr Opin Biotech 2008;19:534–40.
[3] Lutolf MP, Gilbert PM, Blau HM. Designing materials to direct stem-cell fate. Nature 2009;462:433–41.
[4] Mooney DJ, Vandenburgh H. Cell delivery mechanisms for tissue repair. Cell Stem Cell 2008;2:205–13.
[5] Freyman T, Polin G, Osman H, Crary J, Lu MM, Cheng L, et al. A quantitative, randomized study evaluating three methods of mesenchymal stem cell delivery following myocardial infarction. Eur Heart J 2006;27:1114–22.
[6] Wang CC, Chen CH, Lin WW, Hwang SM, Hsieh PCH, Lai PH, et al. Direct intramyocardial injection of mesenchymal stem cell sheet fragments improves cardiac functions after infarction. Cardiovasc Res 2008;77:515–24.
[7] Terrovitis JV, Smith RR, Marban E. Assessment and optimization of cell engraftment after transplantation into the Heart. Circ Res 2010;106:479–94.
[8] Place ES, Evans ND, Stevens MM. Complexity in biomaterials for tissue engineering. Nat Mater 2009;8:457–70.
[9] Martino S, D'Angelo F, Armentano I, Kenny JM, Orlacchio A. Stem cell-biomaterial interactions for regenerative medicine. Biotechnol Adv 2012;30:338–51.
[10] Franz S, Rammelt S, Scharnweber D, Simon JC. Immune responses to implants - a review of the implications for the design of immunomodulatory biomaterials. Biomaterials 2011;32:6692–709.
[11] Hu WJ, Eaton JW, Tang LP. Molecular basis of biomaterial-mediated foreign body reactions. Blood 2001;98:1231–8.
[12] Sakai T, Li RK, Weisel RD, Mickle DAG, Kim ETJ, Jia ZQ, et al. The fate of a tissue-engineered cardiac graft in the right ventricular outflow tract of the rat. J Thorac Cardiov Sur 2001;121:932–42.
[13] Haraguchi Y, Shimizu T, Sasagawa T, Sekine H, Sakaguchi K, Kikuchi T, et al. Fabrication of functional three-dimensional tissues by stacking cell sheets in vitro. Nat Protoc 2012;7:850–8.
[14] Haraguchi Y, Shimizu T, Yamato M, Okano T. Scaffold-free tissue engineering using cell sheet technology. Rsc Adv 2012;2:2184–90.
[15] Qiu F, Chen YZ, Cheng JQ, Wang C, Xu HY, Zhao XJ. A simple method for cell sheet fabrication using mica surfaces grafted with peptide detergent A(6)K. Macromol Biosci 2010;10:881–6.
[16] Akiyama H, Ito A, Kawabe Y, Kamihira M. Genetically engineered angiogenic cell sheets using magnetic force-based gene delivery and tissue fabrication techniques. Biomaterials 2010;31:1251–9.
[17] Chassepot A, Gao LC, Nguyen I, Dochter A, Fioretti F, Menu P, et al. Chemically detachable polyelectrolyte multilayer platform for cell sheet engineering. Chem Mater 2012;24:930–7.
[18] Hong Y, Yu MF, Weng WJ, Cheng K, Wang HM, Lin J. Light-induced cell detachment for cell sheet technology. Biomaterials 2013;34:11–8.
[19] Tamura A, Kobayashi J, Yamato M, Okano T. Thermally responsive microcarriers with optimal poly(N-isopropylacrylamide) grafted density for facilitating cell adhesion/detachment in suspension culture. Acta Biomater 2012;8:3904–13.
[20] Ko IK, Kato K, Iwata H. A thin carboxymethyl cellulose culture substrate for the cellulase-induced harvesting of an endothelial cell sheet. J Biomat Sci-Polym E 2005;16:1277–91.
[21] Kim DW, Jun I, Lee TJ, Lee JH, Lee YJ, Jang HK, et al. Therapeutic angiogenesis by a myoblast layer harvested by tissue transfer printing from cell-adhesive, thermosensitive hydrogels. Biomaterials 2013;34:8258–68.
[22] Kim SJ, Jun I, Kim DW, Bin Lee Y, Lee YJ, Lee JH, et al. Rapid transfer of endothelial cell sheet using a thermosensitive hydrogel and its effect on therapeutic angiogenesis. Biomacromolecules 2013;14:4309–19.
[23] Jun I, Kim SJ, Lee J-H, Lee YJ, Shin YM, Choi E, et al. Transfer printing of cell layers with an anisotropic extracellular matrix assembly using cell-interactive and thermosensitive hydrogels. Adv Funct Mater 2012;22:4060–9.
[24] Park KM, Jun I, Joung YK, Shin H, Park KD. In situ hydrogelation and RGD conjugation of tyramine-conjugated 4-arm PPO-PEO block copolymer for injectable bio-mimetic scaffolds. Soft Matter 2011;7:986–92.
[25] Jun I, Park KM, Lee DY, Park KD, Shin H. Control of adhesion, focal adhesion assembly, and differentiation of myoblasts by enzymatically crosslinked cell-interactive hydrogels. Macromol Res 2011;19:911–20.
[26] Zhu JM, Marchant RE. Design properties of hydrogel tissue-engineering scaffolds. Expert Rev Med Devic 2011;8:607–26.
[27] Bellis SL. Advantages of RGD peptides for directing cell association with biomaterials. Biomaterials 2011;32:4205–10.
[28] Lee JW, Park YJ, Lee SJ, Lee SK, Lee KY. The effect of spacer arm length of an adhesion ligand coupled to an alginate gel on the control of fibroblast phenotype. Biomaterials 2010;31:5545–51.
[29] Verrier S, Pallu S, Bareille R, Jonczyk A, Meyer J, Dard M, et al. Function of linear and cyclic RGD-containing peptides in osteoprogenitor cells adhesion process. Biomaterials 2002;23:585–96.
[30] Ochsenhirt SE, Kokkoli E, McCarthy JB, Tirrell M. Effect of RGD secondary structure and the synergy site PHSRN on cell adhesion, spreading and specific integrin engagement. Biomaterials 2006;27:3863–74.
[31] Feng YZ, Mrksich M. The synergy peptide PHSRN and the adhesion peptide RGD mediate cell adhesion through a common mechanism. Biochemistry 2004;43:15811–21.
[32] Park KM, Lee Y, Son JY, Bae JW, Park KD. In situ SVVYGLR peptide conjugation into injectable gelatin-poly(ethylene glycol)-tyramine hydrogel via enzyme-mediated reaction for enhancement of endothelial cell activity and neovascularization. Bioconjugate Chem 2012;23:2042–50.
[33] Phelps EA, Enemchukwu NO, Fiore VF, Sy JC, Murthy N, Sulchek TA, et al. Maleimide cross-linked bioactive PEG hydrogel exhibits improved reaction kinetics and cross-linking for cell encapsulation and in situ delivery. Adv Mater 2012;24:64–70. 2.
[34] Kharkar PM, Kiick KL, Kloxin AM. Designing degradable hydrogels for orthogonal control of cell microenvironments. Chem Soc Rev 2013;42:7335–72.
[35] Chen S, Li Y, Guo C, Wang J, Ma JH, Liang XF, et al. Temperature-responsive magnetite/PEO-PPO-PEO block copolymer nanoparticles for controlled drug targeting delivery. Langmuir 2007;23:12669–76.
[36] Fusco S, Borzacchiello A, Netti PA. Perspectives on: PEO-PPO-PEO triblock copolymers and their biomedical applications. J Bioact Compat Pol 2006;21:149–64.
[37] Wojak-Cwik IM, Hintze V, Schnabelrauch M, Moeller S, Dobrzynski P, Pamula E, et al. Poly(L-lactide-co-glycolide) scaffolds coated with collagen and glycosaminoglycans: impact on proliferation and osteogenic differentiation of human mesenchymal stem cells. J Biomed Mater Res Part A 2013;101:3109–22.
[38] Tsai KS, Kao SY, Wang CY, Wang YJ, Wang JP, Hung SC. Type I collagen promotes proliferation and osteogenesis of human mesenchymal stem cells via activation of ERK and Akt pathways. J Biomed Mater Res Part A 2010;94A:673–82.
[39] Du MC, Liang H, Mou CC, Li XR, Sun J, Zhuang Y, et al. Regulation of human mesenchymal stem cells differentiation into chondrocytes in extracellular matrix-based hydrogel scaffolds. Colloid Surf B 2014;114:316–23.
[40] Murphy WL, McDevitt TC, Engler AJ. Materials as stem cell regulators. Nat Mater 2014;13:547–57.
[41] Engler AJ, Sen S, Sweeney HL, Discher DE. Matrix elasticity directs stem cell lineage specification. Cell. 2006;126:677–89.
[42] Guvendiren M, Burdick JA. Stiffening hydrogels to probe short- and long-term cellular responses to dynamic mechanics. Nat Commun 2012;3.
[43] Wen JH, Vincent LG, Fuhrmann A, Choi YS, Hribar KC, Taylor-Weiner H, et al. Interplay of matrix stiffness and protein tethering in stem cell differentiation. Nat Mater 2014;13:979–87.
[44] Tang ZL, Akiyama Y, Yamato M, Okano T. Comb-type grafted poly(N-isopropylacrylamide) gel modified surfaces for rapid detachment of cell sheet. Biomaterials 2010;31:7435–43.
[45] Takahashi H, Nakayama M, Itoga K, Yamato M, Okano T. Micropatterned thermoresponsive polymer brush surfaces for fabricating cell sheets with well-controlled orientational structures. Biomacromolecules 2011;12:1414–8.
[46] Patel NG, Cavicchia JP, Zhang G, Newby BMZ. Rapid cell sheet detachment using spin-coated pNIPAAm films retained on surfaces by an aminopropyltriethoxysilane network. Acta Biomater 2012;8:2559–67.
[47] Ohashi K, Yokoyama T, Yamato M, Kuge H, Kanehiro H, Tsutsumi M, et al. Engineering functional two- and three-dimensional liver systems in vivo using hepatic tissue sheets. Nat Med 2007;13:880–5.
[48] Miyahara Y, Nagaya N, Kataoka M, Yanagawa B, Tanaka K, Hao H, et al. Monolayered mesenchymal stem cells repair scarred myocardium after myocardial infarction. Nat Med 2006;12:459–65.
[49] Obokata H, Yamato M, Tsuneda S, Okano T. Reproducible subcutaneous transplantation of cell sheets into recipient mice. Nat Protoc 2011;6:1053–9.
[50] Jin H, Zhang K, Qiao CY, Yuan AL, Li DW, Zhao L, et al. Efficiently engineered cell sheet using a complex of polyethylenimine-alginate nanocomposites plus bone morphogenetic protein 2 gene to promote new bone formation. Int J Nanomed 2014;9:2179–90.
[51] Yu JS, Tu YK, Tang YB, Cheng NC. Sternness and transdifferentiation of adipose-derived stem cells using L-ascorbic acid 2-phosphate-induced cell sheet formation. Biomaterials 2014;35:3516–26.